Weld Cold Cracking in HAZ of Engineering Carbon and Low Alloy Steel (Report I)[†]

— Behavior of Cracking in the RRC Test of SNCM439 and SK5 —

Fukuhisa MATSUDA*, Hiroji NAKAGAWA**, Hwa Soon PARK***, Toshihiro MURAKAWA*** and Michio YAMAGUCHI****

Abstract

In order to investigate the weld cold cracking of engineering carbon and low alloy steels which is considered to be caused by quenching crack, the fundamental behaviors of this type of cracking were studied by means of the RRC test. HAZ cracking in JIS SNCM439 and JIS SK5 was studied under the conditions of the restraint intensity of about 9.8 to 29.4 kN/mm·mm without preheating utilizing GTA welding with austenitic filler wire to eliminate the effect of diffusible hydrogen in the weldment.

As a result, test materials used in this investigation showed very high crack susceptibility and the stress at crack initiation was about 400 and 270 MPa in SNCM439 and SK5, respectively, irrespective of the restraint intensity. It was confirmed, therefore, that quenching crack is susceptible in the welding of these steels. Additionally, the location of crack initiation had a close relation with liquated grain-boundary in HAZ near fusion boundary.

1. Introduction

Engineering carbon and low alloy steels are now widely used for important members of machine structures, tool steels and bearing steels and so on. It is well known, however, that their weldability is very poor, because of their relatively higher carbon content than weldable high strength steels. One of the reason may be that the trials of welding these steels were done mainly by means of manual shielded-arc welding.[1-7] Recently, owing to the development of new welding technologies, e.g. laser and electron beam welding, the applicability of the new technology to these steels and the weldability have been again studied actively.[8-12]

As well known, one of a serious problem in welding of these steels is high susceptibility to cold cracking in HAZ because of high hardenability. It has been reported[2-5] that another type of cold cracking in addition to hydrogen-induced cold cracking occurs easily. Characteristics of the crack are no incubation period[5] and somewhat higher crack initiation temperature.[2,5] Therefore, in general, it is likely to be thought that this crack has analogy with quenching crack in heat treatment. It is well known that the quenching crack occurs when the stress (or strain) induced by thermal contraction and transformation is higher than fracture stress (or strain). With respect to temperature, it has been said[13] that the quenching crack occurs when martensitic transformation proceeds over about 50%.

However, this type of crack in welding has not been studied well and thus the crack initiation and propagation behaviors in relation to martensitic transformation, the morphological characteristics of crack and the effect of chemical composition have not been clear. Therefore, this study is intended to prevent this type of cracking by revealing the cracking phenomena, mechanism and susceptibility in HAZ of these materials.

In this paper, the behaviors of cracking and the microstructural features of crack are studied by means of the RRC test under the conditions that the effect of diffusible hydrogen is negligible. The reason why the RRC test is used in this experiment is as follow: In the RRC test, the restraint stress increases gradually with the cooling of welds. Moreover, the reduction in restraint stress due to transformation expansion and transformation-induced superplasticity in the materials having lower Ms temperature such as high strength steels can be included for evaluation by the RRC test.[14-16] Therefore, increasing process of the restraint stress can be simulated well depending on the restraint condition and transformation

---

character of the steel in fabrication.

2. Materials Used and Experimental Procedures

2.1 Materials used

Medium carbon Ni-Cr-Mo steel JIS SNCM439 and high carbon steel JIS SK5 were used as base metal. Filler wire used for welding was austenitic stainless steel JIS Y310 in order to eliminate the effect of diffusible hydrogen in HAZ. All of these are commercial steels whose chemical compositions are given in **Table 1**.

Table 1 Chemical compositions of materials used.

Material		Chemical composition (wt.%)								Thickness	Dia.
		C	Si	Mn	P	S	Ni	Cr	Mo	(mm)	(mm)
Base metal	SNCM439	0.40	0.26	0.83	0.007	0.009	1.80	0.82	0.26	25	–
	SK5	0.83	0.34	0.48	0.010	0.007	–	–	–	25	–
Filler wire	Y310	0.09	0.51	1.72	0.025	0.005	20.5	25.8	0.04	–	1.6

2.2 Experimental procedures

The shape and size of the specimen is shown in **Fig. 1**. Two plates were put on a RRC cracking tester of 25 ton capacity with two tab plates, and butted each other with a gap of 1.6 mm to make y-slit, and its setting up is shown in **Fig. 2**. The RRC test was carried out in nearly the same manner reported by Satoh et al.[14,17] The restraint in-
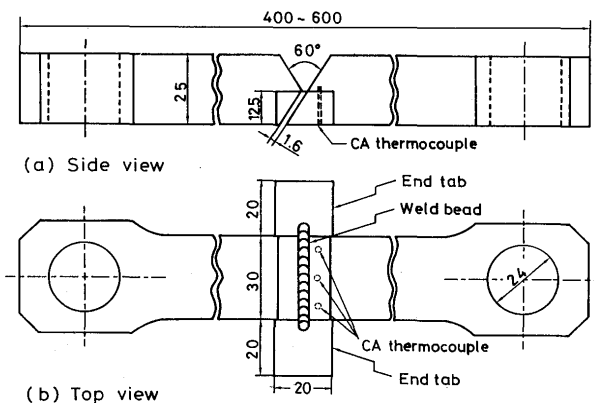

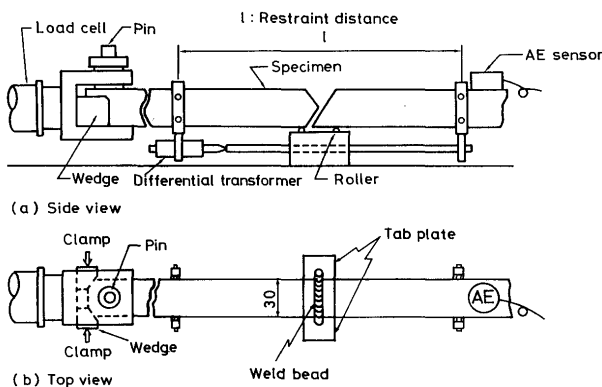**Fig. 1** Configuration of the RRC test specimen.

Fig. 2 Schematic configuration of setting up in the RRC test.

tensity used was three levels of 9.8, 19.6 and 29.4 kN/ mm·mm. By the way, the restraint intensity R_F was calculated by $R_F = Eh/l$ (R; restraint intensity, E; Young's modulus, h; plate thickness, l; restraint length).[17] The restraint stress was calculated by dividing the reaction force by the area of longitudinal crosssection, which was evaluated as the product of bead length and mean throat depth. GTA welding was done with filler wire of Y310 austenitic stainless steel using commercial pure argon shielding gas and constant wire feeding system utilizing welding current of 300A, arc voltage of 19V, welding speed of 2 mm/sec and feeding speed of filler wire of 12.5 mm/sec. The instantaneous change in the selected restraint length l due to the expansion and contraction was detected by a differential transformer and canceled soon under measurement with accuracy of ±0.002 mm. Cooling temperature of HAZ was measured by three CA thermocouples inserted from the back in the three different place along weld bead. Then the cooling temperature curve of the weld was represented by that in the middle of the weld length. Cooling time of $\Delta t_{1073-773K}$ was about 3.5 sec under these welding conditions.

Moreover, acoustic emission technique was applied to detect the crack initiation. The transducer was differential type, which has flat frequency response and has sensitivity of −84 dB referred to 1 V/μbar. Moreover, 100 to 350 kHz bandpass filter was used, and total gain was set to 80 dB.

Besides, the propriety of the AE technique was checked by the tensile cracking test, in which completely the same specimen as in Fig. 1 was set and tensile deformation was applied just after the welding under different crosshead speeds. During this testing, the tensile deformation was removed at various times. After that, five transverse crosssections were observed and correlation between AE and crack was checked.

3. Experimental Results and Discussions

3.1 Behaviors of restraint stress and cracking

Figure 3 shows gradual increase in the restraint stress in the case of base metal SM41, which was done in order to obtain the reference data in the RRC test. The temperature in the ordinate is that measured in the middle of weld length. The restraint stress increases gradually for about first 40 sec immediately after start of welding independent of the restraint intensity (the first step), then is constant (the second step), and again increases gradually to the final value (the third step). The shift to the third step from the second step occurs earlier with increasing the restraint intensity. This tendency agrees well that reported by Satoh et al.[17] By the way, the final value should be changed depending on the restraint intensity in
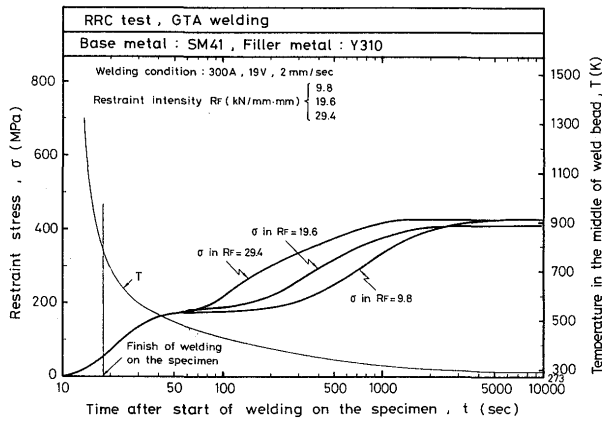
Fig. 3   Behavior of restraint stress in mild steel SM41.

principle. The final values in Fig. 3, however, were nearly constant independent of the restraint intensity. It was thought that the yielding of the weld metal was the reason.

Figures 4(a) and (b) show examples of the behaviors of the restraint stress and AE count rate in SNCM439 and SK5, respectively, under the condition of the restraint intensity of 19.6 kN/mm·mm. In SNCM439 in Fig. 4(a), the first step occurs in the same way as that in SM41. In the second step and the early stage of third step, the
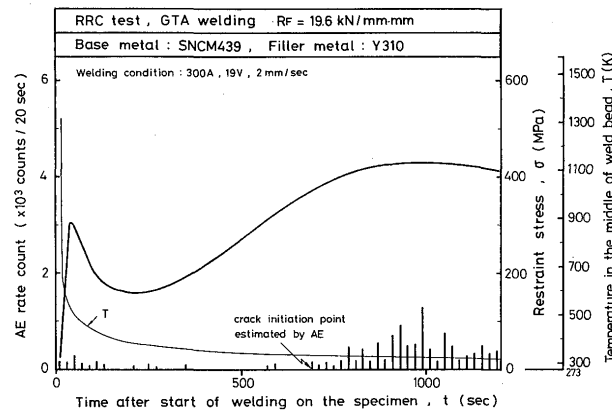
(a) SNCM439
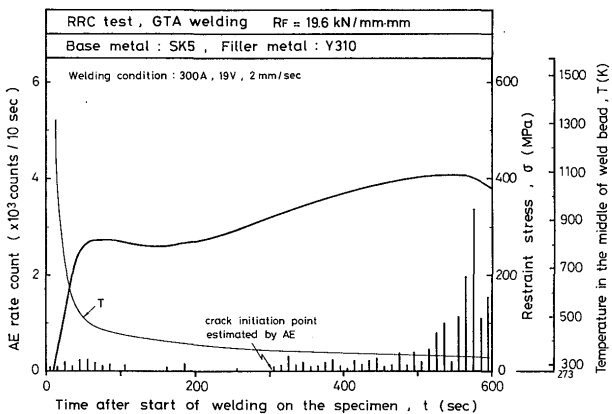
(b) SK5

Fig. 4   Behavior of restraint stress and AE, restraint intensity R_F = 19.6 kN/mm·mm.

restraint stress decreases noticeably due to martensitic transformation, and increases again. Now, it is noticed that the maximum value of the restraint stress in the third step is fairly lower than the final value calculated roughly by the experimental equation[18] even considering the effect of martensitic transformation. As mentioned next, this means that crack occurred and propagated to some extent during the third step.

AE count rate was seen frequently from about 700 sec after the start of welding. The maximum AE count rate occurred when the restraint stress began to decrease after its maximum point. This suggests that crack started from about 700 sec after start of welding. Propriety of such evaluation of crack initiation by AE is mentioned later.

In SK5, the increasing process of the restraint stress is essentially the same as that in SNCM439, with the exception that the reduction of the restraint stress in the second step is less than SNCM439. It was also suggested that the crack initiation time was about 300 sec after the start of welding by AE behavior.

Well, the propriety of the evaluation of crack initiation by AE was confirmed by sudden unloading at different times during the tensile cracking test. The result is shown in Fig. 5, where asterisk means crack initiation point evaluated by AE, solid and open circle mean crack and no crack respectively in the five transverse cross-sections after the unloading. This result confirms that crack initiation time evaluated by AE was resonable.
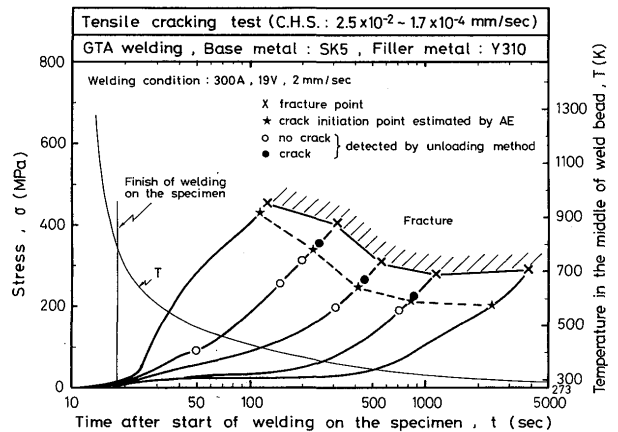

Fig. 5   Experimental confirmation of crack initiation time evaluated with AE technique by sudden unloading method during testing.

Figures 6(a) and (b) show the behaviors of the restraint stress in SNCM439 and SK5, respectively, where asterisk means crack initiation point evaluated by AE technique.

In SNCM439 shown in Fig. 6(a), the restraint stress decreases fairly in the second step due to martensitic transformation, then increases again to the maximum value, and decreases gradually during the third step. This behavior is common in all the restraint conditions. However, it is noteworthy that the crack occurred and pro-

137
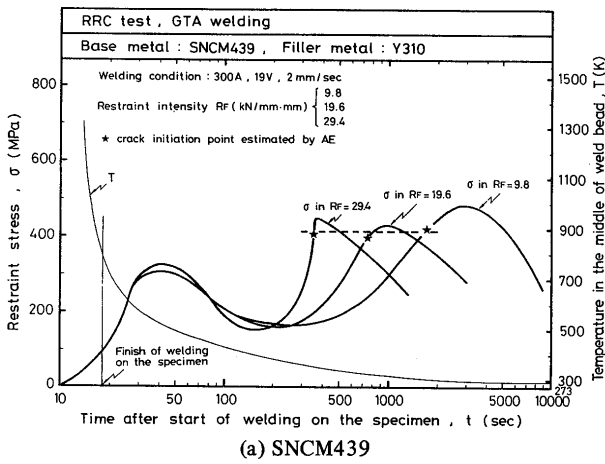
(a) SNCM439
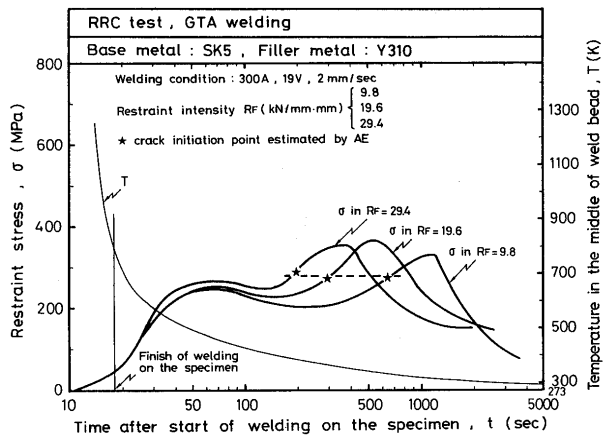
(b) SK5

Fig. 6   Summary of behavior of restraint stress and crack initiation time.

Fig. 7   Relationship between temperature and crack initiation stress.

pagated on the way of the third step even in the lowest restraint intensity. The crack initiation time evaluated by AE was about 1700, 700 and 350 sec after the start of welding in the restraint intensity of 9.8, 19.6 and 29.4 kN/mm·mm, respectively. The restraint stress at the crack initiation was about 400 MPa irrespective of the restraint intensity.

In SK5 shown in Fig. 6(b), the behavior of the restraint stress is nearly the same as that in SNCM439, with the exception that the reduction of restraint stress in the second step is less than that of SNCM439. The crack initiation time was about 650, 290 and 190 sec after the start of welding in the restraint intensity of 9.8, 19.6 and 29.4 kN/mm·mm, respectively. The crack initiation stress was about 270 MPa irrespective of the change of the restraint intensity. SK5 is higher in crack susceptibility than SNCM439 judging from the crack initiation stress and time.

The fact that the crack initiation stress is low in spite of the negligible diffusible hydrogen means that the steels have remarkably high crack susceptibility.

Figure 7 shows the relationship between temperature and crack initiation stress of both steels. The crack initia-
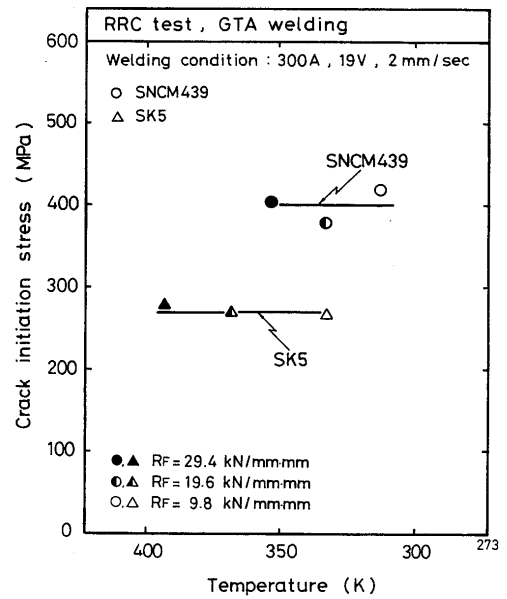
tion stress was nearly the same value irrespective of the restraint intensity or temperature. The crack initiation temperature in the lowest restraint intensity was 313 and 333K in SNCM439 and SK5, respectively. The highest crack initiation temperature was about 353 and 393K in SNCM439 and SK5, respectively, corresponding to the severest restraint intensity. Consequently, it is thought that the crack initiation temperature even in the severest restraint intensity is only a little higher than or nearly the same as that in hydrogen-induced cold cracking.

Figure 8 shows a dilatometric curve during martensitic
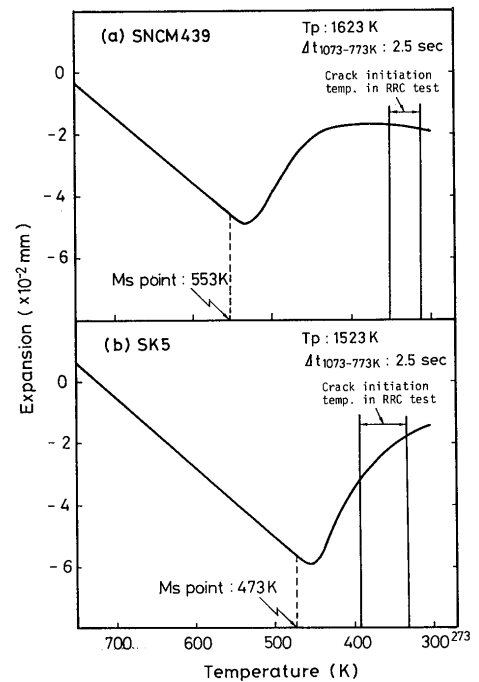

Fig. 8   Dilatometric curve by simulated thermal cycle.

transformation of these steels, in which crack initiation temperature region in the RRC test was shown. Dilatometric curve was measured by simulated thermal cycle testing with high frequency induction heating. Ms temperatures were about 553 and 473K in SNCM439 and SK5, respectively. The region of crack initiation temperature in SNCM439 corresponds to the stage where the martensitic transformation was nearly to be completed, and that in SK5 corresponds to the stage where the martensitic transformation proceeded to about 50%. With respect to the quenching crack in heat treatment, it is considered that generally there has a possibility of cracking at any temperature below Ms temperature. However, the reason why no crack occurred at the temperature near the Ms temperature was thought that the increase in the restraint stress at the third step shifted to long time side i.e., to low temperature side because of the martensitic transformation, as already mentioned.

Figure 9 shows the hardness distribution in HAZ. The maximum hardness was about Hv690 and Hv900 in SNCM439 and SK5, respectively, whose structure in HAZ showed mainly martensite. However, in SK5, troostite was partially observed. The hardened region in SNCM439 is two times as well as than in SK5. By the way, as shown in Fig. 4(a) and (b), the reduction of restraint stress in the second step in SNCM439 was more than that in SK5. This difference is thought to be due to the difference in hardened region in Fig. 9 in spite of the fact that Ms temperature of SK5 is lower than that of SNCM439.
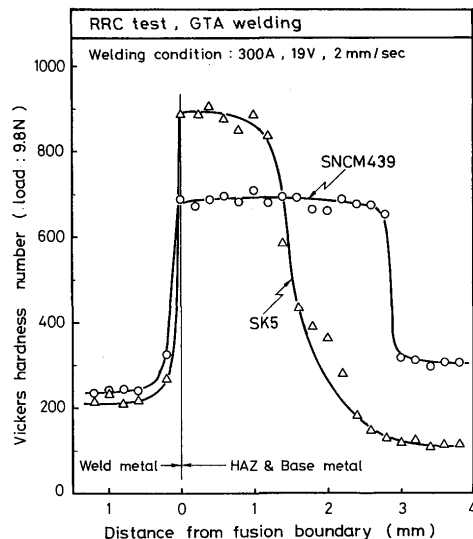

(a) SNCM439

(b) SK5

Fig. 10   Macrostructure of crack in HAZ.

Fig. 11   Microstructure around crack in HAZ of SNCM439.

Fig. 9   Hardness distribution in weldment.

3.2 Macro and microscopic characteristics of crack

Microstructure in HAZ near fusion boundary of these materials was nearly martensite from optical microstructural observation. However, in SK5 troostite was sporadically observed. Weld metal showed austenite. Figures 10 and 11 show typical examples of macro and
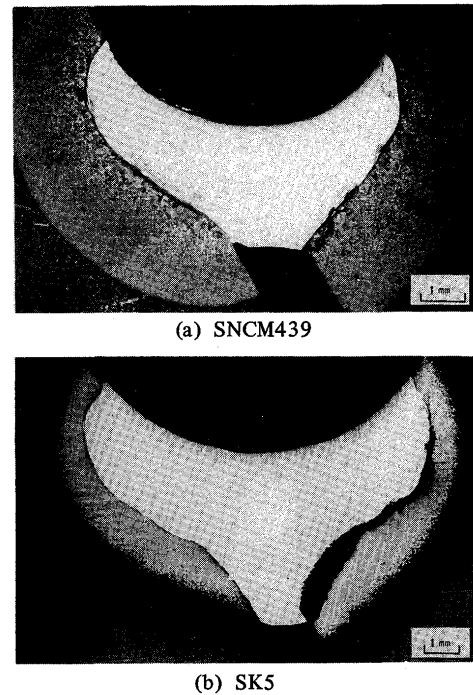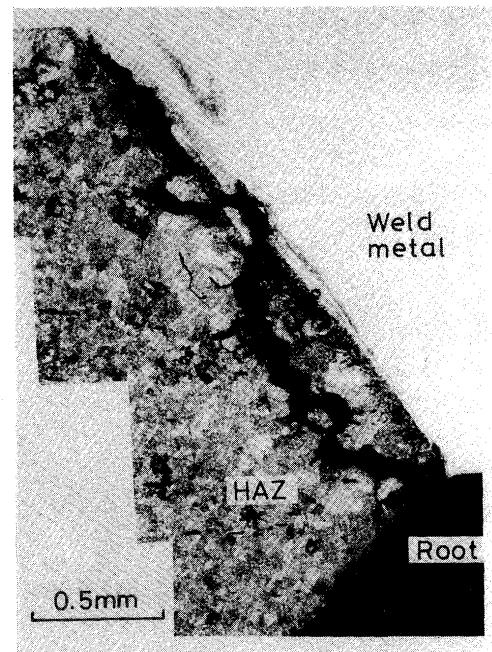
microstructure around crack in the transverse crosssection of weld. As shown in Figs. 10 and 11, crack occurred and propagated in HAZ of coarse grained zone near fusion boundary. Thus, the correlation between the crack and liquated grain-boundary was studied by the aqueous solution with saturated picric acid including wetting agent. According to the result, the traces of grain-boundary liquation was observed around the crack as shown by the arrows in Fig. 12. Therefore, it is concluded that crack initiation part had a close relation with liquated grain-
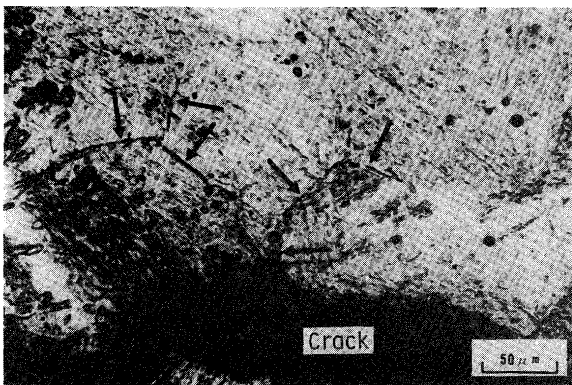
(a) SNCM439

(b) SK5

Fig. 12   Liquated grain-boundary around crack, arrows mean liquated grain-boundary etched with aqueous solution of saturated picric acid including wetting agent.

boundary of coarsed grain in HAZ near fusion boundary.

Microfractographs near the crack initiation part showed typical intergranular fracture surface as shown in **Fig. 13**, and the most of the intergranular facets were very brittle. In crack propagation region, quasi-cleavage fracture surface which was accompanied with considerable plastic deformation was also observed as well as intergranular fracture surface.

4. Conclusions

Main conclusions obtained are as follows:

(1) General behavior of the restraint stress during the RRC test of steels of SNCM439 and SK5 nearly agrees with that of weldable plain carbon steel with the exception of reduction in the restraint stress by martensitic transformation in the second step.

(2) The third step which gives the saturated restraint stress after welding is not seen even in the low restraint intensity of about 10 kN/mm·mm, because the cracking develops somewhat during the third step.

(3) Crack initiation evaluated with AE technique occurs earlier with increasing the restraint intensity. The highest temperature of crack initiation was about 353 and 393K in SNCM439 and SK5, respectively, meaning fairly lower than their Ms temperatures and nearly the same as that in hydrogen-induced cold cracking.

(a) SNCM439
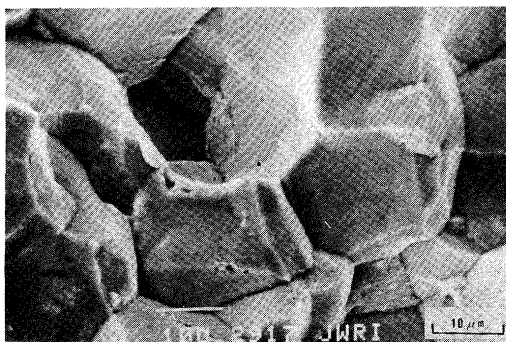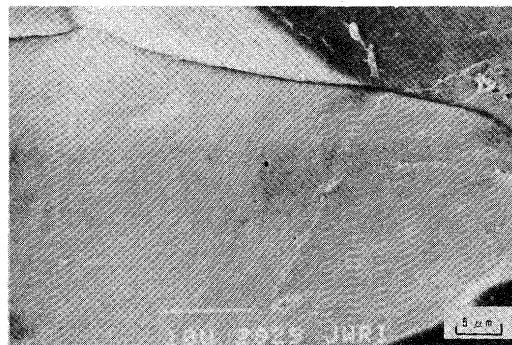
(b) SK5

Fig. 13   SEM microfractograph of intergranular fracture facet in crack initiation part.

(4) The stress at the crack initiation was about 400 and 270 MPa in SNCM439 and SK5, respectively, irrespective of the restraint intensity. Judging from these results, both steels are crack susceptible to cold cracking even in the weldment eliminated diffusible hydrogen. That is to say, they are crack susceptible steels to quenching crack during welding.

(5) Crack initiation part of both steels has a close relation with liquated grain-boundary in HAZ near fusion boundary, and gives very brittle intergranular fracture surface.

References

1) S. Ando and N. Kimata: J. Japan Weld. Soc., 25-6 (1956), 314–321 (in Japanese).

2) K. Notvest: Weld. J., 45-4 (1966), 173s–177s.

3) Y. Nishio et al.: Mitsubishi Juko Giho, 7-4 (1970), 478–486 (in Japanese).

4) M. Kawahara and I. Takahashi: Preprints of the National Meeting of J.W.S., 15 (1971), 22–23 (in Japanese).

5) T. Kobayashi and I. Aoshima: Trans. Japan Weld. Soc., 2-1 (1971), 70–76.

6) F. Matsuda et al.: Trans. JWRI, 7-1 (1978), 71–85.

7) S. Asakura and M. Nihei: Preprints of the National Meeting of J.W.S., 24 (1979), 24-25 (in Japanese).

8) T. Shida et al.: J. Japan Weld. Soc., 49-7 (1980), 440–446 (in Japanese).

9) M. Inagaki et al.: NIRM Report, (1982), 145–162 (in Japanese).

10) A. Shinmi and K. Hara: Weld. Tech. ISSN, 4 (1986), 60–67 (in Japanese).

11) F. Matsuda et al.: Quarterly J. Japan Weld. Soc., 4-1 (1986), 79–83 (in Japanese).

12) N. Sakabata et al.: Quarterly J. Japan Weld. Soc., 4-1 (1986), 131–137 (in Japanese).

13) S. Ohwaku: Netsushori, 7-3 (1967), 140–144 (in Japanese).

14) K. Satoh and S. Matsui: J. Japan Weld. Soc., 36-1 (1967), 29–34 (in Japanese).

15) F. Matsuda et al.: Trans. JWRI, 11-2 (1982), 57–65.

16) F. Matsuda et al.: Trans. JWRI, 13-1 (1984), 47–55.

17) K. Satoh and S. Matsui: J. Japan Weld. Soc., 36-10 (1967), 1096–1109 (in Japanese).

18) H. Suzuki: JWS Bulletin, No. 1 (1976), 54–55 (in Japanese).